Biochemical and Biophysical Research Communications 440 (2013) 762–767

Contents lists available at ScienceDirect

Biochemical and Biophysical Research Communications

journal homepage: www.elsevier.com/locate/ybbrc

New insights into the catalytic mechanism of *Bombyx mori* prostaglandin E synthase gained from structure–function analysis

Kohji Yamamoto [a,*], Mamoru Suzuki [b], Akifumi Higashiura [b], Kosuke Aritake [c], Yoshihiro Urade [c], Nobuko Uodome [c], MD. Tofazzal Hossain [a], Atsushi Nakagawa [b]

[a] Faculty of Agriculture, Kyushu University Graduate School, 6-10-1 Hakozaki, Higashi-ku, Fukuoka 812-8581, Japan
[b] Institute for Protein Research, Osaka University, Suita 565-0871, Japan
[c] Department of Molecular Behavioral Biology, Osaka Bioscience Institute, 6-2-4 Furuedai, Suita, Osaka 565-0874, Japan

ARTICLE INFO

Article history:
Received 25 September 2013
Available online 8 October 2013

Keywords:
Crystal structure
Glutathione
Lepidoptera
Prostaglandin
Prostaglandin synthase

ABSTRACT

Prostaglandin E synthase (PGES) catalyzes the isomerization of PGH_2 to PGE_2. We previously reported the identification and structural characterization of *Bombyx mori* PGES (bmPGES), which belongs to Sigma-class glutathione transferase. Here, we extend these studies by determining the structure of bmPGES in complex with glutathione sulfonic acid (GTS) at a resolution of 1.37 Å using X-ray crystallography. GTS localized to the glutathione-binding site. We found that electron-sharing network of bmPGES includes Asn95, Asp96, and Arg98. Site-directed mutagenesis of these residues to create mutant forms of bmPGES mutants indicate that they contribute to catalytic activity. These results are, to our knowledge, the first to reveal the presence of an electron-sharing network in bmPGES.

1. Introduction

Prostaglandins (PGs) are synthesized from arachidonic acid and influence a variety of physiological and pathological processes in mammalians. There are a number of prostaglandin isomers such as PGH_2, PGD_2, and PGE_2 [1–3]. PGH_2 is an intermediate and is converted by prostaglandin E synthase [PGES, EC 5.3.99.3] to a metabolite, PGE_2. PGES's of mammals are homologs of Sigma-class glutathione transferases [4,5].

The PGES of *Bomyx mori* (bmPGES) is a member of the Sigma-class of glutathione transferases [GSTs, EC 2.5.1.18] [6] that are ubiquitously expressed and function to detoxify diverse xenobiotics and endogenous substances by conjugating them to reduced glutathione (GSH) [7,8]. Multiple classes of GSTs, including Alpha, Mu, Pi, Omega, Sigma, Theta, and Zeta in mammals, are defined according to differences in amino acid sequences [9]. Moreover, Delta, Epsilon, Omega, Sigma, Theta, and Zeta classes have been identified in dipteran insects such as *Anopheles gambiae* and *Drosophila melanogaster* [10]. Because the silkworm is a model animal for studying lepidopteran insects [11,12], which include a number of agricultural pests, comprehensive study of silkworm GSTs will be indispensable for devising strategies for their control.

GST catalyzes a major step in the xenobiotic detoxification pathway. Insect GSTs are of particular interest given their role in insecticide metabolism [13,14]. The silkworm *Bombyx mori* produces Sigma, Omega, Zeta, Delta-class, and unclassified GSTs of [15–20]. Recently, the three-dimensional structures of the Sigma, Omega, Delta-class and unclassified *B. mori* GST were determined [6,21–23]. There are similarities between the structures of bmPGES and prostaglandin D synthase [6]. Because we found that bmPGES converts prostaglandin H_2 into its E_2 form, we were interested in determining the active sites in bmPGES to better understand the structural basis for this activity. Here we report the high resolution (1.37 Å) crystal structure of bmPGES complexed with glutathione sulfonic acid (GTS). Identifying the amino acid residues involved in catalytic function should provide insights into mechanism of prostaglandin E synthase activity, and may facilitate the development of more effective and safe insecticides.

2. Materials and methods

2.1. Protein crystallization and analysis

Recombinant bmPGES was purified according to published methods [6,16,17] that employ ammonium sulfate fractionation,

Abbreviations: GSH, glutathione; GST, glutathione transferase; GSTS, Sigma-class GST; GTS, glutathione sulfonic acid; PG, prostaglandin; PGDS, prostaglandin D synthase; PGES, prostaglandin E synthase; SDS–PAGE, sodium dodecyl sulfate polyacrylamide gel electrophoresis.

* Corresponding author. Address: 6-10-1 Hakozaki, Higashi-ku, Fukuoka 812-8581, Japan. Fax: +81 92 624 1011.
E-mail address: yamamok@agr.kyushu-u.ac.jp (K. Yamamoto).

0006-291X/$ - see front matter © 2013 Elsevier Inc. All rights reserved.
http://dx.doi.org/10.1016/j.bbrc.2013.10.001

ion-exchange chromatography, gel filtration chromatography. The purified enzyme was concentrated using a centrifugal filter (EMD Millipore, Billerica, MA, USA) to approximately 10 mg/ml in 20 mM Tris–HCl buffer, pH 8.5, containing 0.2 M NaCl. Crystallization was performed using the sitting-drop vapor diffusion method at 20 °C using Crystal Screen Kits (Hampton Research, Aliso Viejo, CA, USA) as reservoir solutions. Each drop was formed by mixing an equal (0.2 μl) or two-fold greater volume (0.2:0.4 μl) of protein and reservoir solutions, respectively. Crystals suitable for X-ray analysis were grown for 2 month in 0.1 M HEPES, pH 7.5, 30% PEG400 (w/v), and 20% 1,2-propanediol (v/v), and were then soaked in the same reservoir solution containing 10 mM GTS before analysis. X-ray diffraction data were acquired from analysis of cryo-cooled crystals using synchrotron radiation at beamlines BL-5A at the Photon Factory (The High Energy Accelerator Research Organization, Tsukuba, Japan) and BL44XU in the SPring-8 (Japan Synchrotron Radiation Research Institute (JASRI), Hyogo, Japan) under cryogenic conditions. Crystals were scooped with a nylon loop and frozen in liquid nitrogen. The diffraction data were collected from a single crystal at 90 °K in a stream of nitrogen gas and were processed using *DENZO* and *SCALEPACK* algorithms as implemented in *HKL-2000* software package [24].

2.2. Determination of structure

The molecular replacement method was conducted using *MOLREP* software [25] and the apo-form of bmGSTS1 (PDB ID: 3VPT [6]) as a search model. The structures of bmPGES complexed with GTS were refined using *PHENIX* [26] to analyze data from 50.5 to 1.37 Å. Model rebuilding was performed using *Coot* [27]. The stereochemical quality of the final model was assessed using *MolProbity* [28]. The results of data collection and refinement statistics are summarized in Table 1. Figures were prepared using *PyMOL* (http://pymol.sourceforge.net).

The atomic structure of bmPGES complexed with GTS was deposited in the Protein Data Bank (PDB ID: 3VUR). Alignment of deduced amino acid sequences was performed using GENETYX-MAC (ver. 14.0.12).

2.3. Enzyme assays

Final bmPGES preparations were subjected to SDS–PAGE analysis using a 15% polyacrylamide slab gel containing 0.1% SDS [29] followed by visualization with Coomassie Brilliant Blue R250. Protein concentration was measured using a Protein Assay Kit (Bio-Rad Laboratories, Hercules, CA, USA) with bovine serum albumin as a standard. PGES activity was measured using 10 μM [^{14}C]PGH_2 as substrate in a solution (50 μl) containing 100 mM Tris–HCl, pH 8.0, 1 mM GSH, and 0.1 mg/ml IgG [30]. After incubation at 25 °C for 0.5 min, 300 μl of stop solution (diethylether: methanol: 1 M citric acid = 30:4:1 (by volume)) was added to the reaction mixture, and the organic phase containing fatty acids was dehydrated by adding Na_2SO_4 powder. The products were separated using thin layer chromatography at −20 °C with a diethylether: methanol: acetic acid = 90:2:1 (v/v/v) mobile phase. The conversion rate of ^{14}C-labeled substrate to ^{14}C-labeled products was calculated using a radioimaging plate system (Fujifilm, Tokyo, Japan). GST activity using 1-chloro-2,4-dinitrobenzene (CDNB) and GSH levels were measured spectrophotometrically [6]. Changes in absorbance (340 nm/min) were monitored at 30 °C and converted into moles CDNB conjugated/min/mg protein using the molar extinction coefficient (ε340 = 9600 M^{-1} cm^{-1}) of the product 2,4-dinitrophenyl-glutathione.

Table 1
Data collection and refinement statistics.

Parameter	bmPGES-GTS
Space group	$P6_522$
Unit cell parameters (Å)	$a = b = 57.4$, $c = 209.7$
(°)	$\alpha = \beta = 90$, $\gamma = 120$
Beam line	Photon factory BL-5A
Wavelength (Å)	1.0
Resolution range (Å)	50.5–1.37 (3.69–1.36)
Total number of observation reflections	904,421
Total number of unique reflections	44,634 (1738)
Multiplicity	20.3 (14.7)
R_{merge}[a] (%)	5.6 (40.4)
$\langle I\rangle/\langle\sigma(I)\rangle$[b]	34.4 (4.8)
Completeness (%)	98.6 (100.0)
Refinement statistics	
Resolution range (Å)	27.7–1.37
Number of reflections	
Working set/test set	71,808/3615
R_{work}[c] (%)/R_{free}[d] (%)	15.6/18.2
Root-mean-square deviations	
Bond lengths (Å)/bond angles (°)	0.013/1.6
Average B-factors (Å^2)/number of atoms	
Protein	18.2/3259
Small molecules[e]	24.0/76
Water	30.0/278
Ramachandran analysis	
Preferred regions (%)	97.5
Allowed regions (%)	2.0
Outliers (%)	0.5

[a] $R_{merge} = \sum(I-\langle I\rangle)/\sum\langle I\rangle$, where I is the intensity measurement for a given reflection and $\langle I\rangle$ is the average intensity for multiple measurements of this reflection.
[b] Values in parentheses indicate the highest-resolution shell.
[c] $R_{work} = \sum|F_{obs}-F_{cal}|/\sum F_{obs}$, where F_{obs} and F_{cal} are observed and calculated structure-factor amplitudes.
[d] R_{free} value was calculated using only an unrefined, randomly chosen subset of reflection data (5%) that were excluded from refinement.
[e] Small molecules include GTS, and polyethylene glycol.

2.4. Site-directed mutagenesis

Site-directed mutagenesis of a plasmid containing the coding sequences of wild-type bmPGES was performed using the QuickChange Site-Directed Mutagenesis Kit (Agilent Technologies, Wilmington, DE, USA) according to the manufacturer's recommendations. The nucleotide sequence of the full-length mutant cDNA was determined.

3. Results and discussion

3.1. Structural determination and refinement

The bmPGES monomer comprises N-terminal and C-terminal domains [6]. The N-terminal domain contains the GSH-binding site (G-site), and the C-terminal domain contains the binding site for hydrophobic substrate and PGH_2 (H-site). The diversity at the G- and the H-sites of GST determines substrate selectivity [13,14].

In the present study, we determined the tertiary structure of bmPGES at high resolution (1.37 Å). The crystallographic space group is $P6_522$ with unit cell dimensions of $a = b = 57.4$ Å, and $c = 209.7$ Å. The final X-ray diffraction data and structural refinement statistics are presented in Table 1. Values of $R_{work} = 15.6\%$ and $R_{free} = 18.2\%$ were determined for the refined model with resolutions between 50.5 Å and 1.37 Å. Root-mean-square deviations for bond lengths and angles were 0.013 Å and 1.6°, respectively. Ramachandran analysis showed that 97.5% of the dihedral angles were present in the most preferred regions, 2.0% in the allowed regions, and 0.5% in the outlier regions.

3.2. Amino acid residues involved in GTS-binding

Comparison of unliganded and liganded bmPGES structures did not reveal detectable changes in the main and side chains of bmPGES (Fig. 1). Analysis using Superpose [31] shows structural similarity between apo-bmPGES and GTS-bmPGES with a root-mean-square deviation of 0.885 Å/203 residues (all residues), whereas that between apo-bmPGES and GSH-bmPGES was 0.445 Å/195 residues (all residues) [6]. The deviation between Cα carbons between of apo-bmPGES and GTS-bmPGES was 0.349 Å/203 residues, suggesting that ligand binding did not significantly affect the three-dimensional fold. GTS bound to the G-site was located in the deep cleft between the two domains (Fig. 1). One molecule of GTS bound the active site of each bmPGES monomer (Fig. 1).

The GTS-bmPGES structure indicates that the GTS formed hydrogen bonds with residues Tyr8, Trp39, Lys43, Gln50, Met51, Gln63, and Ser64 (Fig. 1). GSH bound to six of seven residues (Tyr8, Trp39, Lys43, Gln50, Met51, and Ser64) [6]. We identified a residue, Gln63, which interacts with the γ-glutamyl region of GTS forming hydrogen bonds with a water molecule. GTS interacts with its γ-glutamyl moiety to form hydrogen bonds with the side chains of Gln63, the hydroxyl group, and the main chain of Ser64 (Fig. 1). The cysteinyl moiety of GTS forms hydrogen bonds with the main chain of Met51 and the hydroxyl group of Tyr8 (Fig. 1). The glycyl moiety of GTS that interacts with the side chain of Lys43 contacts the side chain of Trp39 (Fig. 1).

3.3. Residues that contribute to the electron-sharing network

An electron-sharing network is essential for glutathione ionization in reactions catalyzed by GSTs [32]. In *Anopheles dirus* glutathione transferase D3–3, the configuration of the glutamyl α-carboxylate group of glutathione, together with the G-site residues Ser-65, Arg-66, Asp-100, Thr-158, and Thr-162 comprise a possible an electron-sharing network that distributes the charge of either a proton or an electron. Electrostatic interaction between the GSH glutamyl and carboxylic Glu64 as well as with Arg66 and Asp100 extends the electron-sharing motif identified previously [32]. This network comprises a functionally conserved motif and can be divided into types I and II [32].

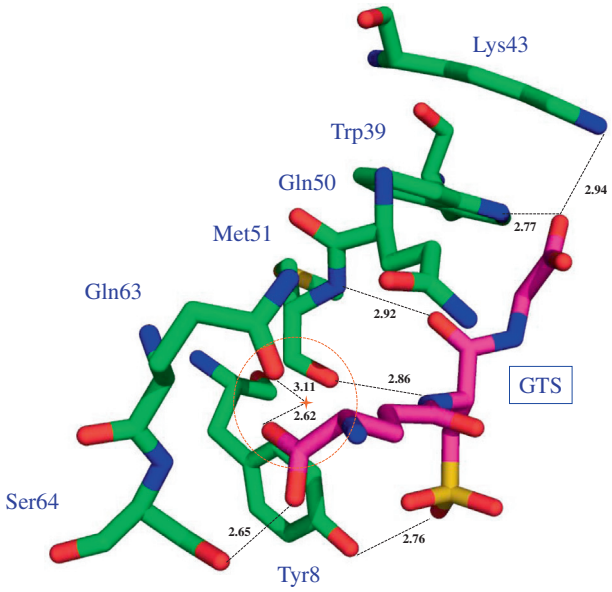

Fig. 1. Amino acid residues near the GSH binding site of bmPGES. Carbon atoms in bmPGES and GTS are green and magenta, respectively. Colors of other atoms are as follows: oxygen (red), nitrogen (blue), and sulfur (yellow). Hydrogen bonds are indicated by black dotted lines. The dotted lines within the orange circle indicate hydrogen bonds formed with a water molecule (orange star). (For interpretation of the references to colour in this figure legend, the reader is referred to the web version of this article.)

The type I electron-sharing networks exemplified by the GSTs of delta, theta, omega and tau classes contain an acidic amino acid residue at position 64, whereas the type II networks (GSTs of alpha, mu, pi and sigma classes) include a polar amino acid residue (Glu) capable of interacting with the γ-glutamyl moiety of GSH. Gln63 is conserved in the sequence of bmPGES, which resembles a member of the type II network and interacts with the γ-glutamyl moiety of GTS through hydrogen bond formation with a water molecule. Further, bmPGES-Asp97 may participate in an ionic interaction characteristic of type II networks.

A stereo view of the electron-sharing type II network of GST (human Pi hGSTP1-1) [32] shows that the type II network contains Arg13, Gln64, Ser65, Glu97, Asp98, and Cys101 in human Pi hGSTP1-1, which superimpose upon Leu14, Gln63, Ser64, Asn96, Asp97, and Arg99 in bmPGES. Analysis of the high-resolution structure of bmPGES, reveals Asn96, Asp97, and Arg99 as putative electron-sharing network residues (Fig. 2). To determine the residues that contribute to catalytic activity via the electron-sharing network in bmPGES, three residues were each converted to Ala using site-directed mutagenesis to create the mutants designated N96A, D97A, and R99A. Proteins purified from *Escherichia coli* migrated as a single band upon SDS–PAGE. The specific activities of the bmPGES mutants were compared with those of the wild-type enzyme using PGH_2 (Fig. 4A) and 1-chloro-2,4-dinitrobenzene (CDNB) (Fig. 4B). Compared with wild-type, the specific activities of all mutant proteins for PGH_2 and CDNB were significantly reduced. In a previous study, Ala substitutions for Leu14, Gln63, and Ser64 of bmPGES exhibited reduced PGES and GST activities [6]. The mutations disrupted the electron distribution network and may have caused the loss from the network of several stabilizing hydrogen bonds. Our present results suggest that these residues form an electron-sharing network for the distribution of a charge requiring either a proton or an electron. Similar results were obtained for Pi-class GSTs in that mutations of amino acid residues forming electron-sharing network altered catalysis [33]. The replacement of Arg15, which is a structural component of the electron-sharing network in the human alpha-class GST (hGSTA1–1), caused a significant reduction in specific activity [34].

Other crystal structures for Sigma-class GST from fruit fly (PDB ID: 1M0U), squid (2GSQ), and human (3EE2) were used to compare electron-sharing networks. Fruit fly GST possesses identical amino acid residues, whereas three of six residues are conserved in squid GST (Arg13, Gln62, Ser63, Gln95, Asp96, and Asn99) and in human GST (Arg14, Gln63, Ser63, Asp96, Asp97, and Ser100). Gln63, Ser64, and Asp97 of bmPGES were identical in other Sigma-class GSTs. The side chain of Gln63 interacts directly with the γ-glutamyl moiety of GSH (Fig. 1) similar to those of the electron-sharing type II networks of Alpha, Mu, Pi and Sigma-class GSTs.

3.4. Putative substrate binding sites

The active site of prostaglandin D synthase (H-PGDS) expressed by hematopoietic cells comprises three pockets (Pockets 1, 2 and 3) [5,35]. In human H-PGDS, Met11, Trp104, Ala105, Leu199, and GSH form Pocket 1, Gly13, Arg14, Met99, and Tyr152 form Pocket 2, and Lys107, Gln109, Lys112, and Lys198 form Pocket 3. The superposition of the backbones of bmPGES and human H-PGDS reveal that bmPGES possesses the three pockets. We found that 11 residues, including Pocket 1 (Val10, Tyr106, and Leu203), Pocket 2 (Ala12, Leu13, Arg98, and Val154), and Pocket 3 (Lys108, Glu110, Lys113, and Glu202) of bmPGES correspond to those of human H-PGDS. The structure of human HPGDS complexed with its

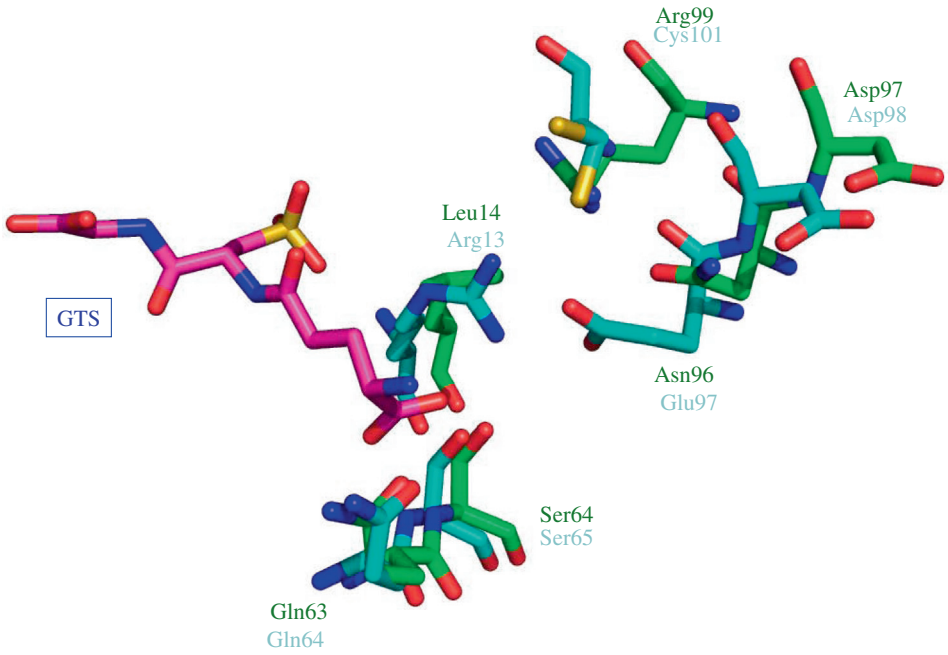

Fig. 2. Superimposed structures of bmPGES and hGSTP1-1 showing amino acid residues of the electron-sharing network. The coloring schemes for bmPGES and GSH are as described in the legend of Fig. 1. The carbon atoms of the amino acid residues of hGSTP1-1 are cyan, except for the regions of oxygen (red), nitrogen (blue), and sulfur (yellow). Symbols of amino acid residues for bmPGES and hGSTP1-1 are shown in green and cyan, respectively. (For interpretation of the references to colour in this figure legend, the reader is referred to the web version of this article.)

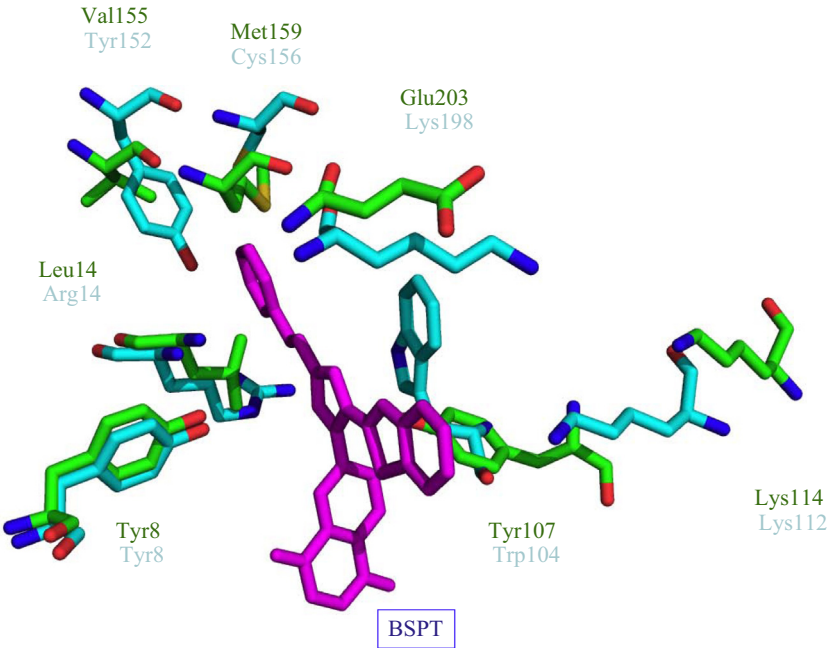

Fig. 3. Putative BSPT-binding site. Carbon atoms in bmPGES and H-PGDS are green and cyan, respectively. BSPT is shown in magenta. Oxygen, nitrogen, and sulfur atoms are red, blue, and yellow, respectively. Symbols of amino acid residues of bmPGES and hGSTP1-1 are green and cyan, respectively. (For interpretation of the references to colour in this figure legend, the reader is referred to the web version of this article.)

inhibitor 2-(2′-benzothiazolyl)-5-styryl-3-(4′-phthalhydrazidyl) tetrazolium chloride (BSPT) (PDB ID: 1V40) has been determined [35]. BSPT interacts with amino acid residues Tyr8, Arg14, Trp104, Lys112, Tyr152, Cys156, and Lys198 [35]. Superposition of human HPGDS with bmPGES reveals that the equivalent bmPGES residues are Tyr8, Leu14, Tyr107, Lys114, Val155, Met159, Glu203 (Fig. 3). The Lys113 residue of bmPGES is located 10.19 Å from the inhibitor. The stacking interaction of BSPT with Tyr106 was observed in the structure of bmPGES (Fig. 3). Tyr106 of bmPGES (Tyr104 in human HPGDS) occupies Pocket 1. The structures of HPGDS complexed with inhibitors such as 4-benzhydryloxy-1-[3-(1*H*-tetrazol-5-yl)-propyl]-piperidine, cibacron blue and 1-amino-4-(4-aminosulfonyl) phenyl-anthraquinone-2-sulphonic acid were determined [35,36]. Superposition of bmPGES with these structures show that they are located within the active site pockets of bmPGES (data not shown). Four residues (Tyr107, Cys110,

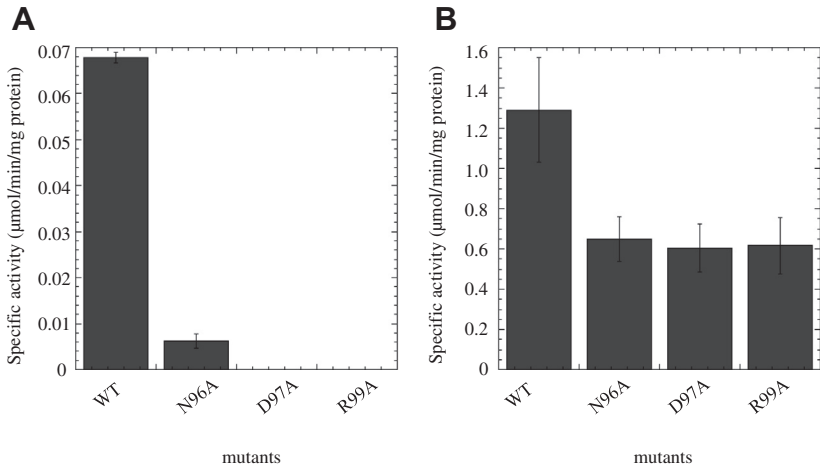

Fig. 4. Specific activities of bmPGES mutants in reactions with PGH_2 (A) and CDNB (B). The activities of wild-type (WT) and mutants (N96A, D97A, and R99A) are shown. Data represent the mean values of three independent experiments.

Phe112, and Cys113) were proposed to reside in the active site of microsomal PGES type 2 [37], although they are not conserved in the amino acid sequence of bmPGES.

In vertebrates, PGE_2 controls biological activities such as smooth muscle dilation and contraction [3], body temperature [2], and the physiological sleep–wake cycle [1]. In invertebrates, PGE_2 signaling is involved in the immune response and oogenesis [38,39]. Thus, the structure of the inhibitor complex of bmPGES may be helpful for the further development of novel insecticides that specifically inhibit PGE_2 production.

In summary, we describe here the crystal structure of a bmPGES complexed with GTS at high resolution (1.37 Å). By preparing complexes and generating mutant enzymes, we identified the amino acid residues involved in the type II electron-sharing network with GSH required for the catalytic activity of bmPGES. The putative substrate-binding sites were conserved in bmPGES. We are currently pursuing cocrystallization of bmPGES with a suitable inhibitor-GSH conjugate to aid in the rational design of more effective pesticides.

Acknowledgments

This work was supported in part by a Grant-in-Aid for Scientific Research from the Ministry of Education, Science, Sports and Culture of Japan. This work was performed under the auspices of the Cooperative Research Program of Institute for Protein Research, Osaka University. The synchrotron radiation experiments were carried out at the BL-5A of Photon Factory (Proposal No. 2012G001 and 2012G003) and at the BL44XU of SPring-8 with the approval of JASRI (Proposal No. 2012A6756, and 2012B6756).

References

[1] O. Hayaishi, Molecular mechanisms of sleep–wake regulation: roles of prostaglandins D2 and E2, FASEB J. 5 (1991) 2575–2581.
[2] A.S. Milton, S. Wendlandt, Effects on body temperature of prostaglandins of the A, E and F series on injection into the third ventricle of unanaesthetized cats and rabbits, J. Physiol. 218 (1971) 325–336.
[3] W.L. Smith, L.J. Marnett, D.L. DeWitt, Prostaglandin and thromboxane biosynthesis, Pharmacol. Ther. 49 (1991) 153–179.
[4] T. Tanioka, Y. Nakatani, N. Semmyo, M. Murakami, I. Kudo, Molecular identification of cytosolic prostaglandin E2 synthase that is functionally coupled with cyclooxygenase-1 in immediate prostaglandin E2 biosynthesis, J. Biol. Chem. 275 (2000) 32775–32782.
[5] Y. Kanaoka, H. Ago, E. Inagaki, T. Nanayama, M. Miyano, R. Kikuno, Y. Fujii, N. Eguchi, H. Toh, Y. Urade, O. Hayaishi, Cloning and crystal structure of hematopoietic prostaglandin D synthase, Cell 90 (1997) 1085–1095.
[6] K. Yamamoto, A. Higashiura, M. Suzuki, K. Aritake, Y. Urade, N. Uodome, A. Nakagawa, Crystal structure of a *Bombyx mori* sigma-class glutathione transferase exhibiting prostaglandin E synthase activity, Biochim. Biophys. Acta 2013 (1830) 3711–3718.
[7] I. Listowsky, M. Abramovitz, H. Homma, Y. Niitsu, Intracellular binding and transport of hormones and xenobiotics by glutathione-S-transferases, Drug Metab. Rev. 19 (1988) 305–318.
[8] R.N. Armstrong, Structure, catalytic mechanism, and evolution of the glutathione transferases, Chem. Res. Toxicol. 10 (1997) 2–18.
[9] B. Mannervik, P.G. Board, J.D. Hayes, I. Listowsky, W.R. Pearson, Nomenclature for mammalian soluble glutathione transferases, Methods Enzymol. 401 (2005) 1–8.
[10] C.P. Tu, B. Akgul, Drosophila glutathione S-transferases, Methods Enzymol. 401 (2005) 204–226.
[11] K. Mita, M. Morimyo, K. Okano, Y. Koike, J. Nohata, H. Kawasaki, K. Kadono-Okuda, K. Yamamoto, M.G. Suzuki, T. Shimada, M.R. Goldsmith, S. Maeda, The construction of an EST database for *Bombyx mori* and its application, Proc. Natl. Acad. Sci. USA 100 (2003) 14121–14126.
[12] K. Mita, M. Kasahara, S. Sasaki, Y. Nagayasu, T. Yamada, H. Kanamori, N. Namiki, M. Kitagawa, H. Yamashita, Y. Yasukochi, K. Kadono-Okuda, K. Yamamoto, M. Ajimura, G. Ravikumar, M. Shimomura, Y. Nagamura, I.T. Shin, H. Abe, T. Shimada, S. Morishita, T. Sasaki, The genome sequence of silkworm, *Bombyx mori*, DNA Res. 11 (2004) 27–35.
[13] D. Fournier, J.M. Bride, M. Poirie, J.B. Berge, F.W. Plapp Jr., Insect glutathione S-transferases. Biochemical characteristics of the major forms from houseflies susceptible and resistant to insecticides, J. Biol. Chem. 267 (1992) 1840–1845.
[14] X. Li, M.A. Schuler, M.R. Berenbaum, Molecular mechanisms of metabolic resistance to synthetic and natural xenobiotics, Annu. Rev. Entomol. 52 (2007) 231–253.
[15] K. Yamamoto, P. Zhang, F. Miake, N. Kashige, Y. Aso, Y. Banno, H. Fujii, Cloning, expression and characterization of theta-class glutathione S-transferase from the silkworm, *Bombyx mori*, Comp. Biochem. Physiol. B Biochem. Mol. Biol. 141 (2005) 340–346.
[16] K. Yamamoto, P.B. Zhang, Y. Banno, H. Fujii, Identification of a sigma-class glutathione-S-transferase from the silkworm, *Bombyx mori*, J. Appl. Entomol. 130 (2006) 515–522.
[17] K. Yamamoto, H. Fujii, Y. Aso, Y. Banno, K. Koga, Expression and characterization of a sigma-class glutathione S-transferase of the fall webworm, *Hyphantria cunea*, Biosci.Biotechnol. Biochem. 71 (2007) 553–560.
[18] K. Yamamoto, S. Nagaoka, Y. Banno, Y. Aso, Biochemical properties of an omega-class glutathione S-transferase of the silkmoth, *Bombyx mori*, Comp. Biochem. Physiol. C Toxicol. Pharmacol. 149 (2009) 461–467.
[19] K. Yamamoto, Y. Shigeoka, Y. Aso, Y. Banno, M. Kimura, T. Nakashima, Molecular and biochemical characterization of a Zeta-class glutathione S-transferase of the silkmoth, Pestic. Biochem. Physiol. 94 (2009) 30–35.
[20] K. Yamamoto, H. Ichinose, Y. Aso, Y. Banno, M. Kimura, T. Nakashima, Molecular characterization of an insecticide-induced novel glutathione transferase in silkworm, Biochim. Biophys. Acta 2011 (1810) 420–426.
[21] Y. Kakuta, K. Usuda, T. Nakashima, M. Kimura, Y. Aso, K. Yamamoto, Crystallographic survey of active sites of an unclassified glutathione transferase from *Bombyx mori*, Biochim. Biophys. Acta 2011 (1810) 1355–1360.
[22] K. Yamamoto, K. Usuda, Y. Kakuta, M. Kimura, A. Higashiura, A. Nakagawa, Y. Aso, M. Suzuki, Structural basis for catalytic activity of a silkworm Delta-class glutathione transferase, Biochim. Biophys. Acta 2012 (1820) 1469–1474.
[23] K. Yamamoto, M. Suzuki, A. Higashiura, A. Nakagawa, Three-dimensional structure of a *Bombyx mori* Omega-class glutathione transferase, Biochem. Biophys. Res. Commun. 438 (2013) 588–593.

[24] Z. Otwinowski, W. Minor, Processing of X-ray diffraction data collected in oscillation mode, Methods Enzymol. 276 (1997) 307–326.
[25] A. Vagin, A. Teplyakov, An approach to multi-copy search in molecular replacement, Acta Crystallogr. D Biol. Crystallogr. 56 (2000) 1622–1624.
[26] P.D. Adams, P.V. Afonine, G. Bunkoczi, V.B. Chen, N. Echols, J.J. Headd, L.W. Hung, S. Jain, G.J. Kapral, R.W. Grosse Kunstleve, A.J. McCoy, N.W. Moriarty, R.D. Oeffner, R.J. Read, D.C. Richardson, J.S. Richardson, T.C. Terwilliger, P.H. Zwart, The Phenix software for automated determination of macromolecular structures, Methods 55 (2011) 94–106.
[27] P. Emsley, K. Cowtan, Coot: model-building tools for molecular graphics, Acta Crystallogr. D Biol. Crystallogr. 60 (2004) 2126–2132.
[28] V.B. Chen, W.B. Arendall 3rd, J.J. Headd, D.A. Keedy, R.M. Immormino, G.J. Kapral, L.W. Murray, J.S. Richardson, D.C. Richardson, MolProbity: all-atom structure validation for macromolecular crystallography, Acta Crystallogr. D Biol. Crystallogr. 66 (2010) 12–21.
[29] U.K. Laemmli, Cleavage of structural proteins during the assembly of the head of bacteriophage T4, Nature 227 (1970) 680–685.
[30] M. Lazarus, B.K. Kubata, N. Eguchi, Y. Fujitani, Y. Urade, O. Hayaishi, Biochemical characterization of mouse microsomal prostaglandin E synthase-1 and its colocalization with cyclooxygenase-2 in peritoneal macrophages, Arch. Biochem. Biophys. 397 (2002) 336–341.
[31] W. Kabsch, C. Sander, Dictionary of protein secondary structure: pattern recognition of hydrogen-bonded and geometrical features, Biopolymers 22 (1983) 2577–2637.
[32] P. Winayanuwattikun, A.J. Ketterman, Glutamate-64, a newly identified residue of the functionally conserved electron-sharing network contributes to catalysis and structural integrity of glutathione transferases, Biochem. J. 402 (2007) 339–348.
[33] K.H. Kong, H. Inoue, K. Takahashi, Site-directed mutagenesis study on the roles of evolutionally conserved aspartic acid residues in human glutathione S-transferase P1-1, Protein Eng. 6 (1993) 93–99.
[34] R. Bjornestedt, G. Stenberg, M. Widersten, P.G. Board, I. Sinning, T.A. Jones, B. Mannervik, Functional significance of arginine 15 in the active site of human class alpha glutathione transferase A1-1, J. Mol. Biol. 247 (1995) 765–773.
[35] T. Inoue, Y. Okano, Y. Kado, K. Aritake, D. Irikura, N. Uodome, N. Okazaki, S. Kinugasa, H. Shishitani, H. Matsumura, Y. Kai, Y. Urade, First determination of the inhibitor complex structure of human hematopoietic prostaglandin D synthase, J. Biochem. 135 (2004) 279–283.
[36] Y. Kado, K. Aritake, N. Uodome, Y. Okano, N. Okazaki, H. Matsumura, Y. Urade, T. Inoue, Human hematopoietic prostaglandin D synthase inhibitor complex structures, J. Biochem. 151 (2012) 447–455.
[37] T. Yamada, J. Komoto, K. Watanabe, Y. Ohmiya, F. Takusagawa, Crystal structure and possible catalytic mechanism of microsomal prostaglandin E synthase type 2 (mPGES-2), J. Mol. Biol. 348 (2005) 1163–1176.
[38] J. Park, D. Stanley, Y. Kim, Rac1 mediates cytokine-stimulated hemocyte spreading via prostaglandin biosynthesis in the beet armyworm, *Spodoptera exigua*, J. Insect Physiol. 59 (2013) 682–689.
[39] M.N. Medeiros, R. Belmonte, B.C. Soares, L.N. Medeiros, C. Canetti, C.G. Freire-de-Lima, C.M. Maya-Monteiro, P.T. Bozza, I.C. Almeida, H. Masuda, E. Kurtenbach, E.A. Machado, Arrest of oogenesis in the bug *Rhodnius prolixus* challenged with the fungus *Aspergillus niger* is mediated by immune response-derived PGE2, J. Insect Physiol. 55 (2009) 150–157.